

AMMRC MS 68-10

**STRAIN-HARDENING AND INTERACTION EFFECTS
ON THE GROWTH OF VOIDS IN DUCTILE
FRACTURE***

**Monograph Series by
*DENNIS M. TRACEY***

November 1968

This document has been approved for public release and sale; its distribution is unlimited.

**D/A Project 1C024401A349
AMCMS Code 5025.11.299
Materials Research for Specific Army Requirements
Subtask 39171**

*Research partially funded by U. S. Atomic Energy Commission under Contract AT(30-1)-2394 with Brown University, Providence, Rhode Island.

**APPLIED MECHANICS RESEARCH LABORATORY
ARMY MATERIALS AND MECHANICS RESEARCH CENTER
WATERTOWN, MASSACHUSETTS**

CONTENTS

	Page
ABSTRACT	
INTRODUCTION	1
FORMULATION OF PROBLEM	2
BOUNDING THE FLOW STRESS	7
SOLUTION OF INTEGRAL EQUATION FOR AN INFINITE BODY WITH A CONSTANT VOID GROWTH RATE	8
SOLUTION OF INTEGRAL EQUATION FOR AN INFINITE BODY WITH A CONSTANT IMPOSED STRESS STATE	12
VOID GROWTH IN THE NECK OF A TENSILE SPECIMEN	20
DISCUSSION	25
ACKNOWLEDGMENT	27
REFERENCES	28

ARMY MATERIALS AND MECHANICS RESEARCH CENTER

STRAIN-HARDENING AND INTERACTION EFFECTS ON
THE GROWTH OF VOIDS IN DUCTILE FRACTURE

ABSTRACT

The growth and coalescence of voids is a common mechanism of fracture in ductile materials. Analytical work on the problem to date has dealt mainly with isolated voids in perfectly plastic materials, so that strain hardening and interactions between neighboring voids have been neglected. These features of void growth are examined here, but only for a simple geometrical configuration. In particular, the growth of single infinitely long cylindrical voids in bodies of rigid-plastic, strain-hardening material is considered. Bodies with both finite and infinite dimensions normal to the void surface are included in the analysis. The exact relation among the pertinent variables: transverse stress, axial strain, hardening coefficient, void strain and void growth rate is presented. Solution via a bounding technique is given for two general cases. The first case is that of an imposed constant void growth rate and the second case is an imposed constant transverse stress. The results show a decelerating effect of hardening on void growth. Application to the ductile fracture problem of void growth in the neck of a tensile specimen demonstrates the accelerating effect of void growth due to interactions between voids.

Introduction

Ductile fracture as a consequence of the growth and coalescence of voids has been observed by many experimenters including Rogers [1]^{*}, Gurland and Plateau [2], and Bluhm and Morrissey [3]. Voids nucleate by the cracking of inclusions, the decohesion of inclusions from the matrix, and reportedly also in the matrix metal near the inclusions [2]. McClintock and O'Day [4] discount the importance of the last nucleation site in their finding that dislocations have a small effect on fracture strain of the bubble-raft analogue of a crystal. Once the voids appear they grow and coalesce by the plastic deformation of the matrix which in this paper is considered a problem in continuum plasticity. McClintock [5] justifies this approach as reasonable when the inclusions in the material are large enough to be seen under an optical microscope.

The fracture of a simple tension specimen commences with the nucleation of fine cracks and voids in the necked region along the axis. Rogers [1] states that the flat portion of the cup and cone fracture is a direct consequence of the coalescence of voids which have grown under the influence of the prevailing triaxial stress system. The voids are most dense at the axis of the neck where the triaxiality of stress is greatest indicating a direct relation between void nucleation and growth and triaxiality.

The analytical approach to the problem is not obvious because the mechanism of coalescence is not understood. A first attempt would ignore the interaction between voids and consider each void as growing in an infinite domain until the radius has grown to one-half the spacing between voids. McClintock [6] used

* The numbers in square brackets refer to the list of references at the end of this report.

this approach in his void growth work. The approach in this paper again ignores interaction as such but considers each void as in its own secluded domain of transverse dimension equal to the average spacing between voids. At some small void density it is valid to consider the void domains as infinite; as growth proceeds the effects of the void growth will be "felt" in the neighboring voids' domains so that finite body analysis begins as an approximate method of describing the acceleration in growth due to the interaction.

There has been no published work known to the writer which solves exactly the problem of interaction of voids (however, McClintock [5] presented an approximate analysis of coalescence by shear bands between voids); in fact, there has not been any work reported on the exact solution of non-interacting voids in strain-hardening materials. McClintock [6] presented a criterion of ductile fracture by the growth of non-interacting voids in infinite domains of rigid strain-hardening material. The void growth behavior for the strain-hardening material is not exact however; it is obtained from an extrapolation between the behavior in perfect plastic and viscous materials. Rice and Tracey [7] presented a variational treatment of void growth in infinite domains of any rigid plastic material but only perfect plastic applications were presented. Hence an exact strain-hardening treatment is desirable and here presented.

Formulation of Problem

In a previous paper [7] the growth of isolated cylindrical and spherical voids in infinite bodies of perfectly plastic material was treated. Here the growth of a cylindrical void in "finite" (infinite length and finite transverse

dimensions) and infinite bodies of rigid-plastic, strain-hardening material is considered, Fig. 1. The bodies are cylindrical in shape with an axis of infinite length and a radius b , b having any value, finite or infinite. A cylindrical void of radius r_o is oriented along the z direction of the (r, θ, z) polar coordinate system defined in Fig. 1. A strain is imposed on the body in the axial direction at a rate $\dot{\epsilon}$ while the radial stress $(\sigma_r)_b$ is applied at the external radius b . The axial direction is the direction of maximum principal stress and strain-increment in all cases considered. The problem lies in finding the expansion of the void as a function of the imposed stress and strain.

The incompressibility condition gives the velocity field [7] :

$$\begin{aligned}\dot{u}_r &= -\frac{r}{2} \dot{\epsilon} + \frac{r_o^2}{r} \left(\frac{\dot{\epsilon}}{2} + \frac{\dot{r}_o}{r_o} \right) \\ \dot{u}_z &= \dot{\epsilon} z \\ \dot{u}_\theta &= 0.\end{aligned}\tag{1}$$

The void growth rate \dot{r}_o/r_o must be known to completely specify the velocity field. Note that at large values of r the velocity at r is not influenced by the value of \dot{r}_o/r_o . If the body has a large enough radial dimension so that the void growth is not "felt" at some large value of r within the body, then the body can be considered infinite.

The relation among void growth rate, imposed stress and strain, and strain history is formulated through the equation of equilibrium

$$\frac{\partial \sigma_r}{\partial r} + \frac{\sigma_r - \sigma_\theta}{r} = 0\tag{2}$$

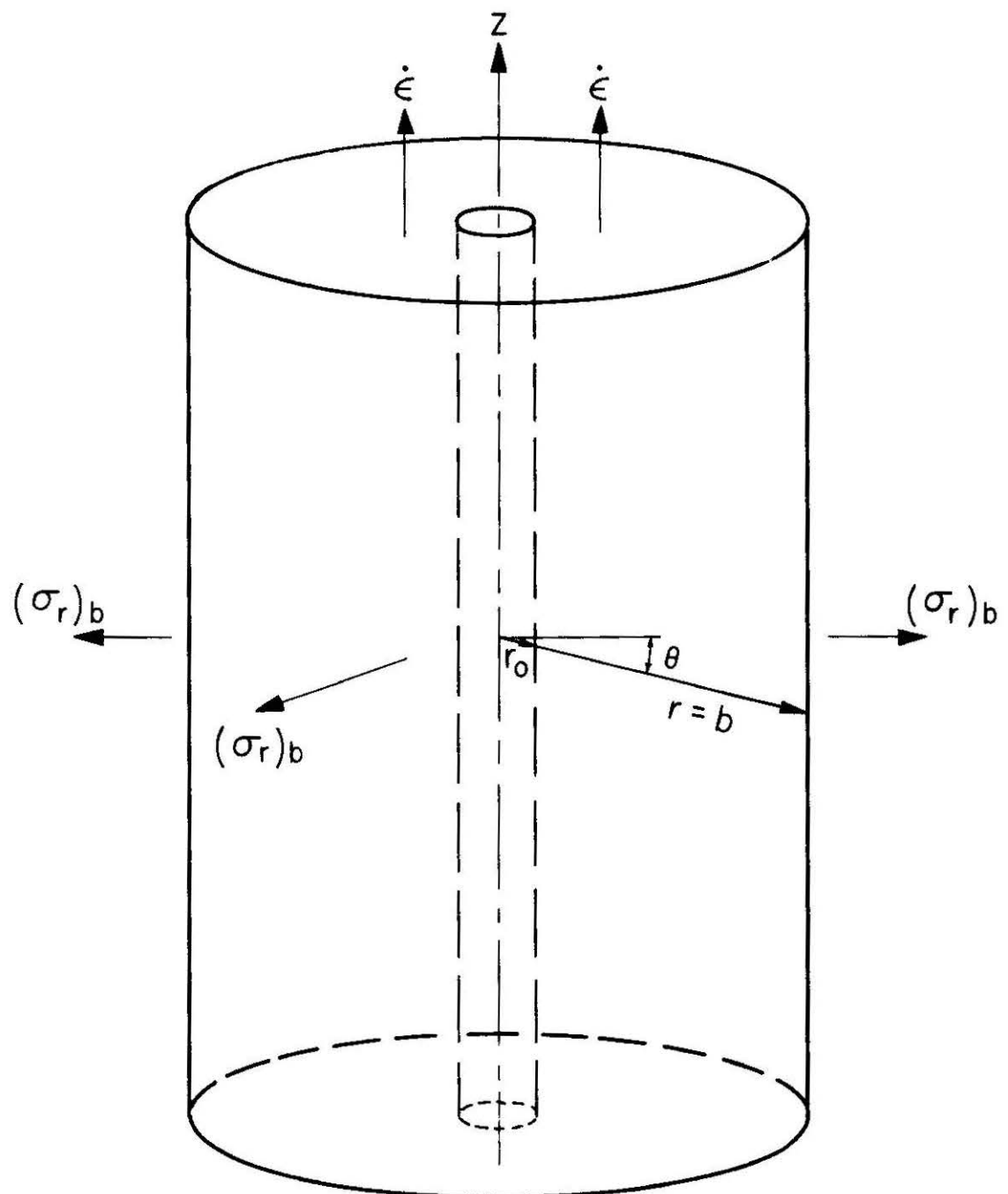


FIG. I CYLINDRICAL VOID IN BODY UNDER IMPOSED STRESS AND STRAIN-RATE.

and the stress-incremental strain relation which for an isotropic Mises material is

$$s_{ij} = \sqrt{2} \tau \frac{\dot{\epsilon}_{ij}}{\sqrt{\dot{\epsilon}_{kl} \dot{\epsilon}_{kl}}} \quad (3)$$

where s_{ij} is the deviatoric stress tensor, $\dot{\epsilon}_{ij}$ is the strain-rate tensor and τ is the hardening parameter which is a function of the deformation history and equal to the equivalent shear flow stress. Obtaining $\dot{\epsilon}_{ij}$ from eq. (1), substituting into eq. (2), dividing both sides by τ_b (the equivalent shear flow stress at the boundary), and integrating over the body gives

$$(\sigma_r/\tau)_b = 2 \int_{r_o/b}^1 \frac{\tau}{\tau_b} \frac{(\dot{\epsilon} + 2 \frac{\dot{r}_o}{r_o}) \frac{r_o}{r} d(\frac{r_o}{r})}{\sqrt{3\dot{\epsilon}^2 + (\frac{r_o}{r})^4 (\dot{\epsilon} + 2 \frac{\dot{r}_o}{r_o})^2}} . \quad (4)$$

A power law relation between τ and the generalized strain γ is assumed. In Lagrangian coordinates (radial coordinate denoted by R) γ can be written as

$$\gamma(\epsilon, R) = \int_0^\epsilon \dot{\gamma}(n, R) dn \quad (5)$$

where

$$\dot{\gamma} = \sqrt{2\dot{\epsilon}_{ij} \dot{\epsilon}_{ij}} .$$

The strain-rate field $\dot{\epsilon}_{ij}$ is found from the velocity field eq. (1) in Eulerian coordinates. The relation between Eulerian (r) and Lagrangian (R) coordinates is found through incompressibility:

$$(r/r_o)^2 = \frac{1}{1+e} \int_0^{\epsilon} (1+2 \frac{\dot{r}_o}{r_o}) d\eta \left[\left(\frac{R}{R_o} \right)^2 - 1 \right] . \quad (6)$$

Using eq. (6) to obtain $\dot{\gamma}(R)$ and subsequently transforming back to Eulerian coordinates to obtain $\gamma(r)$ and substituting into eq. (4) with the notation

$$\dot{H} = \dot{\epsilon} + 2 \frac{\dot{r}_o}{r_o}$$

$$H = \epsilon + 2 \ln \left(\frac{r_o}{R_o} \right)$$

$$x = r_o/r$$

gives the final form of the integral equation in $(\sigma_r/\tau)_b$, ϵ , r_o/b , $\dot{\epsilon}$

and \dot{r}_o/r_o

$$(\sigma_r/\tau)_b(\epsilon) = 2 \int_{r_o/b}^1 \left[\frac{\int_0^{\epsilon} \left[\frac{3 + \left[\frac{\dot{H}(\eta)}{1+e^{H(\epsilon)-H(\eta)}} (x^{-2} - 1) \right]}{\gamma_b} \right]^2 d\eta}{\sqrt{3\dot{\epsilon}^2 + x^4 H^2(\epsilon)}} \right]^N \frac{\dot{H}(\epsilon) x dx}{\sqrt{3\dot{\epsilon}^2 + x^4 H^2(\epsilon)}} . \quad (7)$$

Bounding the Flow Stress

The flow stress τ appearing in eq. (7) is a cumbersome quantity. It is a function of position, void strain, imposed strain, and the complete strain history:

$$\tau = \frac{\tau_b}{\gamma_b^N} \left[\int_0^\epsilon \left[3 + \left[\frac{H(n)}{1+e^{H(\epsilon)-H(n)}(x^{-2}-1)} \right]^2 \right]^{1/2} dn \right]^N . \quad (8)$$

In an effort to simplify the problem, bounds to τ were derived by obtaining bounds to γ which hereafter will be called γ^a . γ^a can be written in Eulerian coordinates as

$$\gamma^a = \int_0^\epsilon \sqrt{(\sqrt{3} dn)^2 + \left(\frac{d\beta}{1+b e^{-\beta}} \right)^2} \quad (9)$$

$$\beta = H(n)$$

$$b = e^{H(\epsilon)}(x^{-2}-1) .$$

It can be thought of as the arclength of the actual strain path in ϵ, H space just as

$$s = \int_{o_C}^{x_1, x_2} \sqrt{dx_1^2 + dx_2^2} \quad (10)$$

is the arclength of a path C in x_1, x_2 space. For monotonic paths, paths which have a slope of constant sign,

$$|x_1| + |x_2| \geq s \geq \sqrt{x_1^2 + x_2^2} . \quad (11)$$

This point is illustrated in Fig. 2. The upper bound is a square path while the lower bound is a straight line path. The same bounds can be applied to the arclength of the actual straining path γ^a as long as the straining process gives a monotonic path (of course the path can always be divided into piecewise monotonic portions):

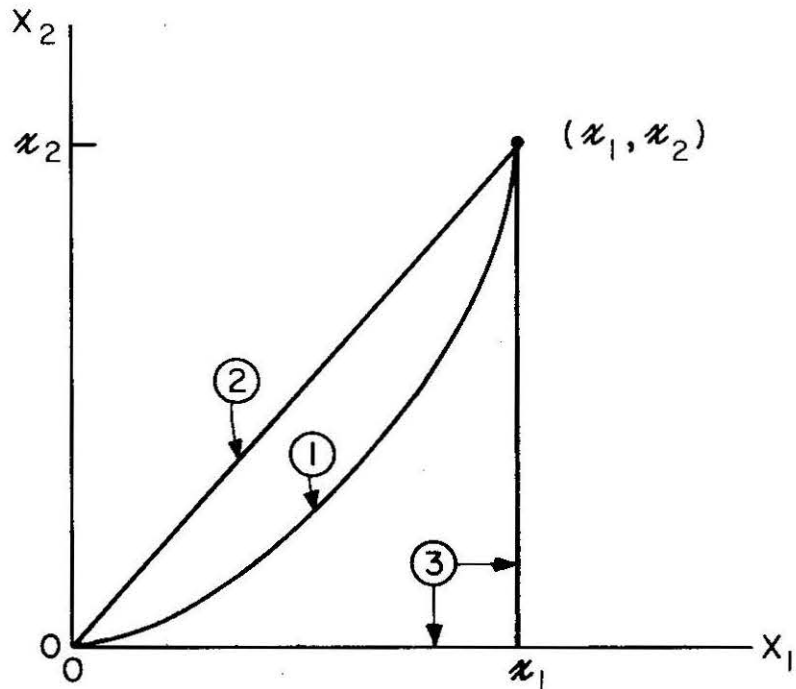
$$\gamma^u = |\sqrt{3} \epsilon| + |\ln((e^{-H(\epsilon)} - 1)x^2 + 1)| \geq \gamma^a \geq \sqrt{3\epsilon^2 + (\ln((e^{-H(\epsilon)} - 1)x^2 + 1))^2} = \gamma^l . \quad (12)$$

The bounds are path independent; this is a very significant simplification from eq. (8). They were employed in the following with a large saving in computation time.

Solution of Integral Equation for an Infinite Body with a Constant Void

Growth Rate

When the void growth rate is constant, $\dot{H} = \text{constant}$, the integral eq. (7) has its simplest form. Although the physical situations in which a constant growth rate is encountered are not numerous, solution of the equation for this case gives a feeling for the void growth behavior with the minimum of computational effort. For convenience, the body containing the void will be chosen to have an infinite radius. The resulting integral equation is



PATH 1 A MONOTONIC PATH BETWEEN $(0,0)$ AND (x_1, x_2)

SIGN $(\frac{dx_2}{dx_1})$ CONSTANT OVER THE PATH

PATH 2 STRAIGHT LINE PATH BETWEEN $(0,0)$ AND (x_1, x_2)

MONOTONIC PATH OF SHORTEST ARC LENGTH

PATH 3 "SQUARE" PATH BETWEEN $(0,0)$ AND (x_1, x_2)

MONOTONIC PATH OF LARGEST ARC LENGTH

FIGURE 2 BOUNDS TO MONOTONIC STRAINING PATHS

$$(\sigma_r/\tau)_\infty(\epsilon) = 2 \int_0^1 \left[\frac{\int_0^\epsilon \left[3 + \left[\frac{\dot{H}}{1+e^{\dot{H}(\epsilon-\eta)}(x^{-2}-1)} \right]^{1/2} \right]^N d\eta}{\sqrt{3} \epsilon} \right] \frac{\dot{H} x dx}{\sqrt{3\dot{\epsilon}^2 + x^4 \dot{H}^2}} . \quad (13)$$

For a given constant value of \dot{H} eq. (13) is solved for $(\sigma_r/\tau)_\infty(\epsilon)$, the stress state at infinity necessary to maintain \dot{H} . For this problem the bounds to γ^a can be applied to obtain bounds to $(\sigma_r/\tau)_\infty(\epsilon)$. By using γ^l a lower bound to $(\sigma_r/\tau)_\infty$ is obtained; by using γ^u an upper bound to $(\sigma_r/\tau)_\infty$ is obtained:

$$(\sigma_r/\tau)_\infty^l(\epsilon) = 2 \int_0^1 \left[\frac{\sqrt{3\dot{\epsilon}^2 + [\ln\{(e^{-\dot{H}(\epsilon)} - 1)x^2 + 1\}]^2}}{\sqrt{3} \epsilon} \right]^N \frac{\dot{H} x dx}{\sqrt{3\dot{\epsilon}^2 + x^4 \dot{H}^2}} \quad (14)$$

$$(\sigma_r/\tau)_\infty^u(\epsilon) = 2 \int_0^1 \left[\frac{\sqrt{3\dot{\epsilon}^2 + |\ln\{(e^{-\dot{H}(\epsilon)} - 1)x^2 + 1\}|^2}}{\sqrt{3} \epsilon} \right]^N \frac{\dot{H} x dx}{\sqrt{3\dot{\epsilon}^2 + x^4 \dot{H}^2}}$$

The quantity $H(\epsilon)$ is known in this problem to equal $H\epsilon$. The cumbersome double integral (13) has been replaced by two single integrals. The computation time of obtaining the bounds to $(\sigma_r/\tau)_\infty(\epsilon)$ is many times smaller than the time necessary to obtain the actual $(\sigma_r/\tau)_\infty(\epsilon)$. Fig. 3 shows how the actual curve (found from solution of eq. (13) falls between the bounds for the constant growth rates of $\dot{r}_o/r_o = 5$ and $10\dot{\epsilon}$.

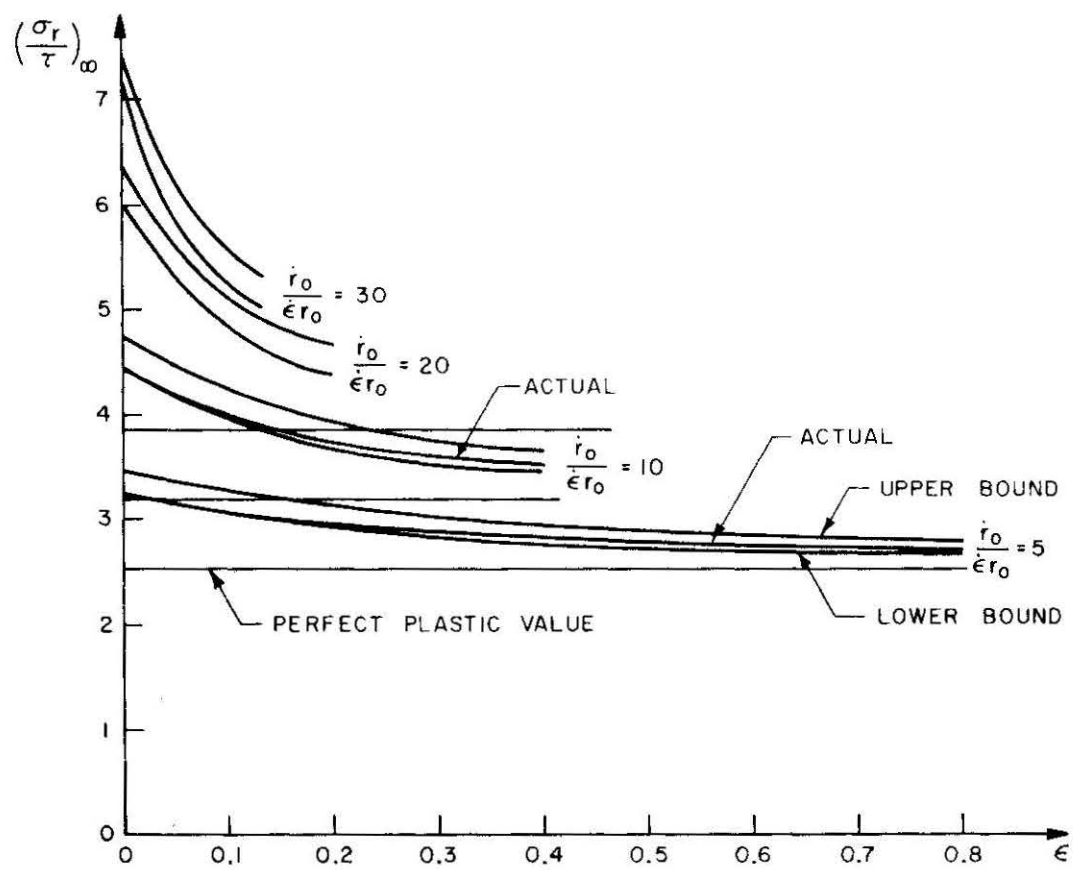


FIG. 3 BOUNDS TO $(\sigma_r / \tau)_\infty [\epsilon]$ FOR IMPOSED GROWTH RATES OF 5, 10, 20, 30. $N = .3$.

Plots of $(\sigma_r/\tau)_\infty^{u,\ell}$ are given in Fig. 4 for growth rates of 5, 10, 20 and $30\dot{\epsilon}$ for $N = .1$. Fig. 3 is the same for $N = .3$. The curves were calculated to values of ϵ which would cause a geometric strain of the void equal to fifty.

It is interesting that the stress state required to maintain the imposed growth rate asymptotically decreases to the value required if the material were perfectly plastic ($N = 0$). The deviation from the perfectly plastic stress state at a value of ϵ decreases with value of imposed growth rate and hardening coefficient. This suggests that for situations which induce small growth rates, in the order of $\dot{\epsilon}$, perfect plasticity would be an acceptable idealization. This point is demonstrated in the last section. Another implication of the curves of Figs. 3-4 is that if the stress state were imposed constant, the void growth rate would continually increase to the perfectly plastic growth rate. The next section investigates this possibility.

Solution of Integral Equation for an Infinite Body with a Constant Imposed Stress State

When the imposed stress state is constant the integral eq. (7) has the form

$$k = \int_0^1 \frac{\tau(\epsilon, H(n), x)}{\tau_\infty} g(H(\epsilon), x) dx \quad (15)$$

where k is the imposed stress $(\sigma_r/\tau)_\infty$. The yield stress τ depends upon the imposed strain ϵ , position x , and the entire history of the void strain which is represented by $H(n)$. The problem is to obtain the function $H(n)$ or

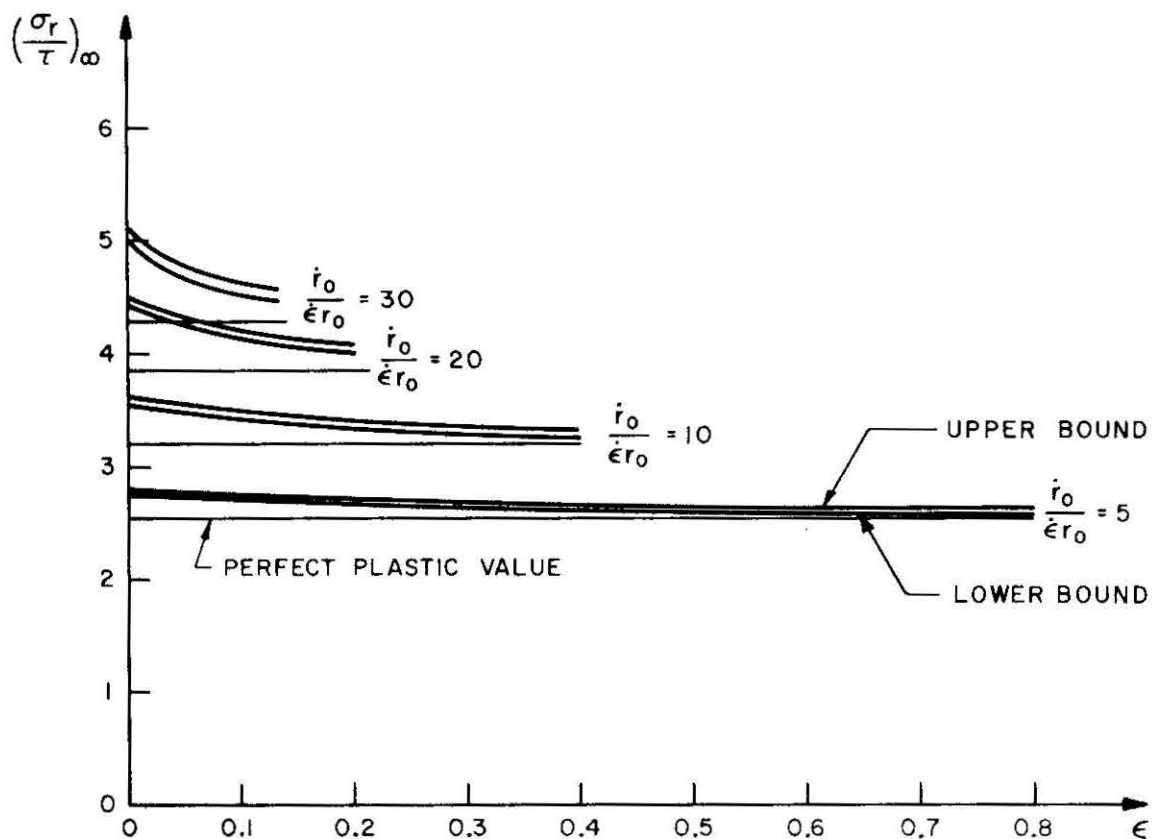


FIG. 4 BOUNDS TO $(\sigma_r/\tau)_\omega$ [ϵ] FOR IMPOSED GROWTH RATES OF 5, 10, 20, 30. $N=1$

just as well $\dot{H}(\eta)$ which gives $H(\eta)$ upon integration. Again bounds to τ will be employed.

The proportional strain and "square" strain bounds to the actual strain path will be used to release τ of its path dependence:

$$\tau^l(\epsilon, H(\epsilon), x) \leq \tau(\epsilon, H(\eta), x) \leq \tau^u(\epsilon, H(\epsilon), x) \quad (16)$$

where τ^l and τ^u are from eq. (12). The use of τ^l would render an upper bound to $\dot{H}(\epsilon)$ while τ^u would render a lower bound to $\dot{H}(\epsilon)$ if $\tau^{u,l}$ could be evaluated. They cannot be evaluated since they depend upon $H(\epsilon)$, the intrinsic unknown of the problem. Since the derivatives of τ^l and τ^u with respect to $H(\epsilon)$ are positive, bounds to $\dot{H}(\epsilon)$ can still be obtained by replacing $H(\epsilon)$ in τ^l with some lower bound, $H^l(\epsilon)$, and replacing $H(\epsilon)$ in τ^u with some upper bound, $H^u(\epsilon)$. The resulting bounds on $\dot{H}(\epsilon)$, \dot{H}^u and \dot{H}^l , will bound the bounds that would result from the use of $H(\epsilon)$ in τ^u, τ^l . Obvious candidates for $H^u(\epsilon)$ and $H^l(\epsilon)$ are

$$H^u(\epsilon) = \int_0^\epsilon \dot{H}^u(\eta)d\eta; \quad H^l(\epsilon) = \int_0^\epsilon \dot{H}^l(\eta)d\eta. \quad (17)$$

It should be noted that any bounds to $H(\epsilon)$ can be employed.

Substituting into the integral equation (13) yields two single integral equations:

$$k = 2 \left[\int_0^1 \frac{\sqrt{3\epsilon^2 + (\ln\{(e^{-H^l(\epsilon)} - 1)x^2 + 1\})^2}}{\sqrt{3}\epsilon} d\eta \right]^N \frac{\dot{H}^u(\epsilon) x dx}{\sqrt{3\epsilon^2 + (\dot{H}^u(\epsilon)x)^2}} \quad (18a)$$

$$k = 2 \int_0^1 \left[\frac{\sqrt{3}\epsilon + |\ln\{(e^{-H^u(\epsilon)} - 1)x^2 + 1\}|}{\sqrt{3}\epsilon} \right]^N \frac{\dot{H}^l(\epsilon) x dx}{\sqrt{3\dot{\epsilon}^2 + (\dot{H}^l(\epsilon)x)^2}} . \quad (18b)$$

Equations (18) are two equations in the unknowns $\dot{H}(\epsilon)^u, l$. They are interrelated. The first yields $\dot{H}^u(\epsilon)$ but only after knowing $\dot{H}^l(\epsilon)$ which is found from the second equation by integrating $\dot{H}^l(n)$. Similarly the second equation requires $\dot{H}^u(n)$ before yielding $\dot{H}^l(\epsilon)$.

At $\epsilon = 0$ the exact equation, eq. (15), reduces to

$$k = 2 \int_0^1 \left[\frac{3 + (\dot{H}^a(0)x^2)^2}{3} \right]^{N/2} \frac{\dot{H}^a(0) x dx}{\sqrt{3 + (\dot{H}^a(0)x^2)^2}} . \quad (19)$$

Solving for $\dot{H}^a(0)$ and using it to evaluate $\tau^l(0)$ and $\tau^u(0)$ allows solution of eq. (18) for $\dot{H}(0)^u$ and $\dot{H}(0)^l$. Thereupon the bounds are iteratively evaluated at small increments of ϵ . In the plots presented the increment in ϵ was adjusted with k so as to instigate a void true strain increment of .05. Plots of the bounds to $\dot{r}_o/\dot{\epsilon}r_o$ were obtained for $(\sigma_r/\tau)_\infty$ values of 3, 3.5, 4, and 5.5 for hardening coefficients of .1 and .3, Figs. 5-7. Actual solution of eq. (15) was obtained for imposed stress states of 3 and 5.5, Figs. 6,7.

The spread between bounds is greatest for high stress states. For small imposed stresses like those encountered in the neck of a tensile specimen the

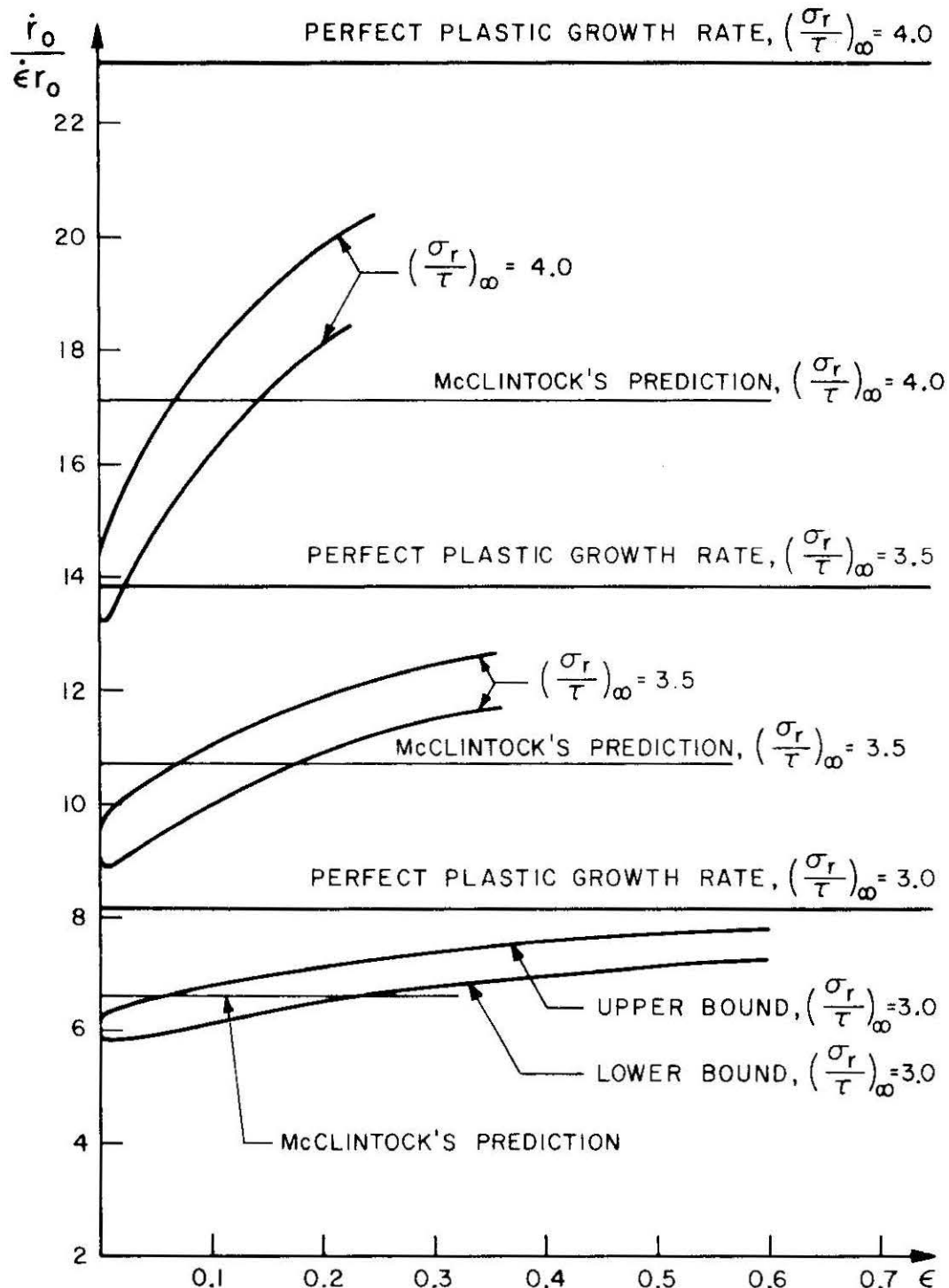


FIG. 5 BOUNDS TO $\dot{r}_0 / \dot{\epsilon}r_0 [\epsilon]$ FOR IMPOSED $(\frac{\sigma_r}{\tau})_\infty$
VALUES OF 3, 3.5, 4. N = .1

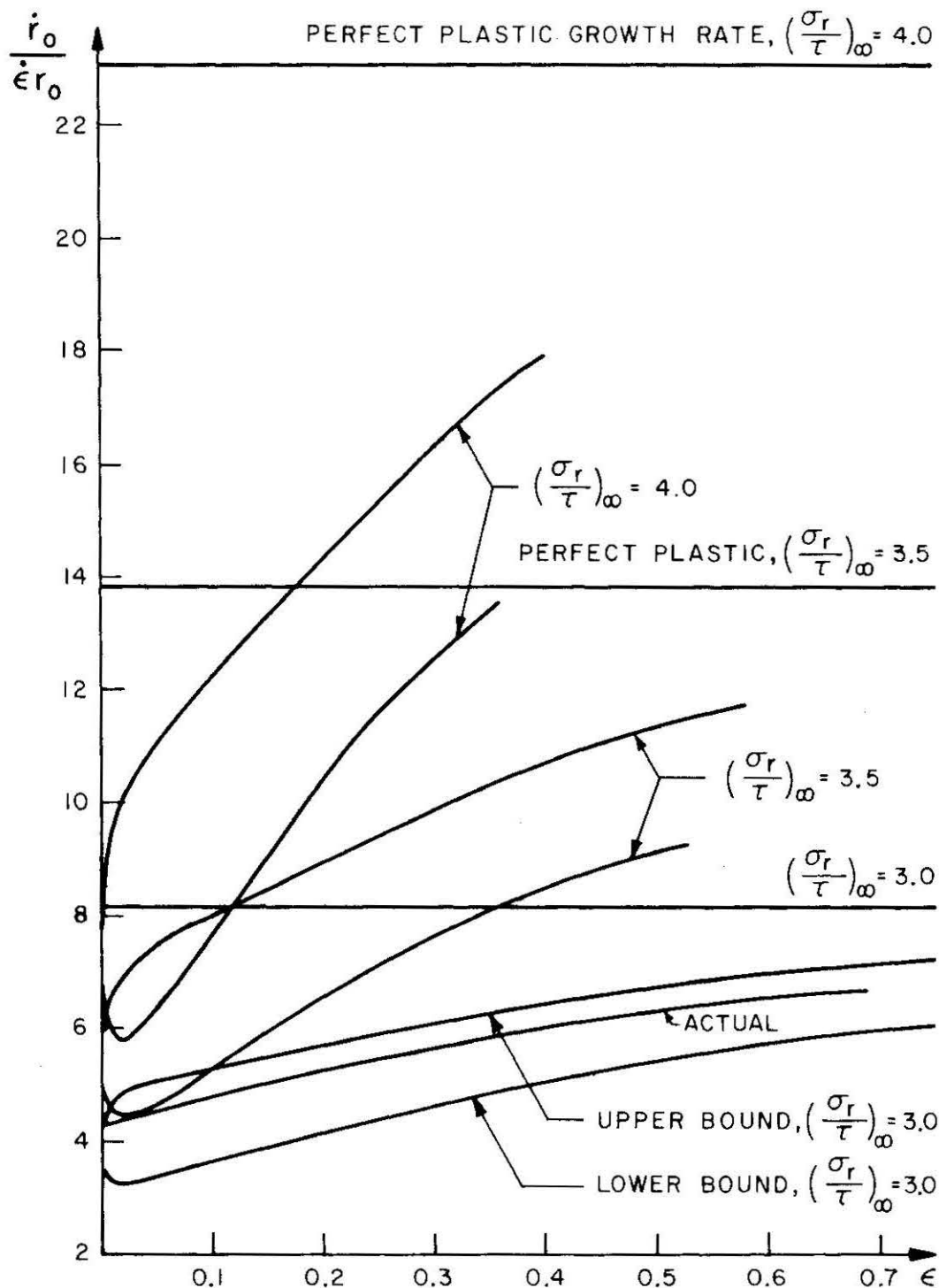


FIG. 6 BOUNDS TO $\dot{r}_0 / \dot{\epsilon} r_0 [\epsilon]$ FOR IMPOSED $(\sigma_r / \tau)_\infty$
VALUES OF 3, 3.5, 4. N = .3

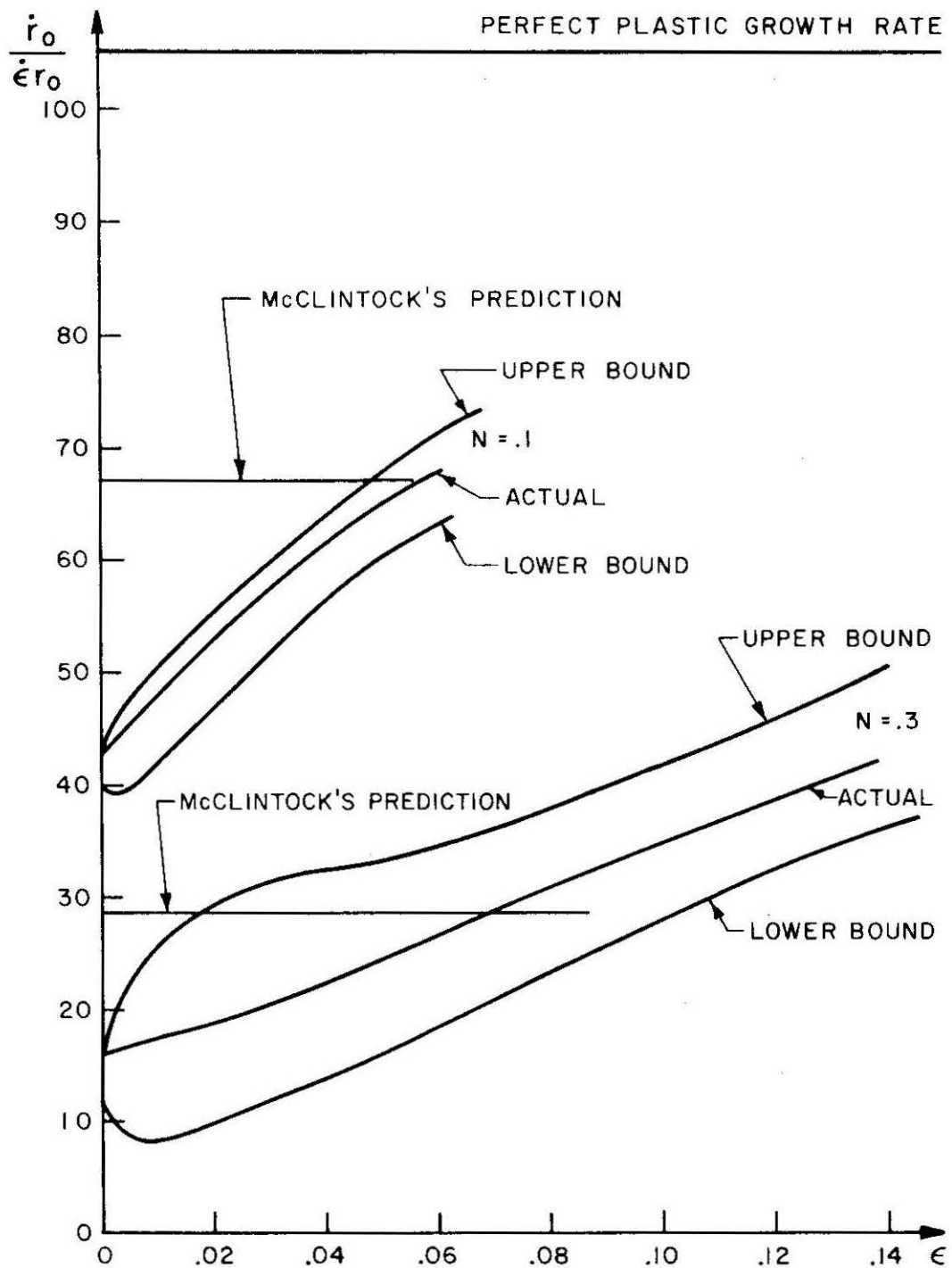


FIG. 7 BOUNDS TO $\frac{r_0}{\dot{\epsilon}r_0} [\epsilon]$ FOR IMPOSED $(\sigma_r / \tau)_\omega$ OF 5.5. $N = .1, .3$. ALSO ACTUAL CURVES.

bounds are very close. In all cases the void growth rate increases asymptotically to the perfect plastic growth rate as the longitudinal strain ϵ increases. The degree to which strain-hardening decelerates void growth is directly related to the degree of triaxiality and the value of the hardening coefficient.

The growth rate predicted from McClintock's approximate work [6] is given in a few cases on Figs. 5,7. His equation (27) for this case of equal transverse stress, put in present notation, relates void growth rate and stress as

$$\dot{r}_o / \epsilon r_o = \frac{1}{2} \left[\frac{\sqrt{3}}{1-n} \sinh \{ (1-n)(\sigma_r / \tau)_\infty \} - 1 \right] .$$

The transient effect of void growth rate with strain ϵ is not included in this approximation, a very important feature as seen in the Figs. 5-7.

When the strain-rate along the axis of the body of Fig. 1 is reversed in direction so that the z-direction becomes the direction of minimum principal stress and strain-rate, the only difference in result from the present case is that the growth ratio is faster by the amount $\dot{\epsilon}$. The integral equation is the same for both cases. The only difference is in the relation between \dot{H} and \dot{r}_o / r_o :

$$\dot{r}_o / r_o = \frac{\dot{H} + \dot{\epsilon}}{2} .$$

The minus sign holds for the present case, the positive sign when $\dot{\epsilon}$ is reversed.

Void Growth in the Neck of a Tensile Specimen

The necking of a tensile specimen introduces triaxiality of stress in the necked region. Bridgman [8] found that the strain was very nearly uniform at the necked section, so that the state of stress in the neck consists of a uniaxial stress equal to the flow stress, $\sqrt{3} \tau$, plus a hydrostatic tension, σ . The latter is given approximately in terms of the neck radius, a , radius of curvature of the neck surface, R , and distance from the axis, r , as

$$\sigma = (\sqrt{3} \tau) \ln(1 + a/2R - r^2/2aR) . \quad (20)$$

In an attempt to predict the ductility of tensile specimens for various initial void densities the interior of the necked region was assumed to contain a number of cylindrical voids of radius r_0 and spacing $2b$, with axes aligned with the tension direction. The initial void diameter to spacing ratio was taken as the cube root of the volume fraction of voids present in the material under consideration. Each void is assumed to grow independently in its own finite domain of radius b . When the void radius grows to a value equal to b there is coalescence and internal fracture is complete; incipient shear, in the scheme of Bluhm and Morrissey [3], follows to finalize the fracture with a comparably small additional strain.

Since voids are seen to be most dense at the axis of the necked region [3], the stress state there will be used as that stress state imposed on the cell walls. To obtain a relation between a/R and the longitudinal true strain ϵ the a/R vs ϵ plot of Bridgman [8] was utilized. The data was collected using steel, bronze, and copper tensile specimens. The spread in data is considerable (as would be expected since the necking process varies with material) but for a

first attempt the relation obtained from fitting a curve to the data was used:

$$\frac{a}{R} = 2.93 [1 - \exp \{-(\epsilon - .1)/3\}] \quad (21)$$

for $\epsilon > .1$.

With this the imposed radial stress can be written as a function of ϵ :

$$\sigma_r(\epsilon) = (\sqrt{3} \tau) \ln \left[1 + \frac{2.93}{2} \{1 - \exp \{-(\epsilon - .1)/3\}\} \right] \quad (22)$$

for $\epsilon > .1$.

The quantity $(\sqrt{3} \tau)$ is the uniaxial flow stress present in the neck along with the hydrostatic stress. Since τ is the flow stress in shear, which is constant across the neck (8), it was evaluated via the power-law relationship from the strain state far from the void conglomeration at the axis:

$$\tau = \tau_\infty \propto (\sqrt{3} \epsilon)^N \quad (23)$$

The integral equation (7) takes the form

$$\begin{aligned} \sqrt{3} \ln \left[1 + \frac{2.93}{2} \{1 - \exp \{-(\epsilon - .1)/3\}\} \right] \\ = 2 \int_{r_o(\epsilon)}^l \left[\frac{\gamma}{\sqrt{3} \epsilon} \right]^N \frac{\dot{H}(\epsilon) x dx}{\sqrt{3\epsilon^2 + x^4 H^2(\epsilon)}} \quad (24) \end{aligned}$$

The void spacing is changed only by the nominal transverse strain

$$b(\epsilon) = b(0) \exp \{-\epsilon/2\}$$

so that the radius ratio is given by

$$\frac{r_o}{b}(\epsilon) = \frac{r_o}{b}(0) \exp \left\{ \frac{1}{2} \int_0^\epsilon H(n) dn \right\} . \quad (25)$$

The hardening coefficient of a material is influenced by the density of inclusions, particles and voids. The data of Edelson and Baldwin [9] relating N and the volume portion of second phase particles (including voids) of two-phase copper-base alloys was used in this analysis. The bounds to γ , eq. (12), can be utilized with the modification of using bounds to $H(\epsilon)$ as in the previous section. The equations were solved for initial void volume fractions of 0.02 to 0.2. The fracture strain, ϵ^f , at which the voids coalesce is that strain when $r_o/b = 1$. In practice at some radius ratio less than 1 the growth rate takes a sudden surge which implies coalescence at the next increment of strain. The radius ratio just before coalescence varied between 2/3 and 3/4. The resulting ductility-volume fraction curve is plotted in Fig. 8 along with the experimental curve of Edelson and Baldwin [9], the curve offered by McClintock [5], and the solution of eq. (24) for the case $b = \infty$. Except at small volume fractions all the curves predict ductilities much larger than those experimentally observed. Certainly there have been many simplifications made which might cause the discrepancy. Voids of all shapes are oriented in all directions in the center of a tensile specimen neck. The increase in volume fraction of voids with applied strain due to both void growth and continued void nucleation must be

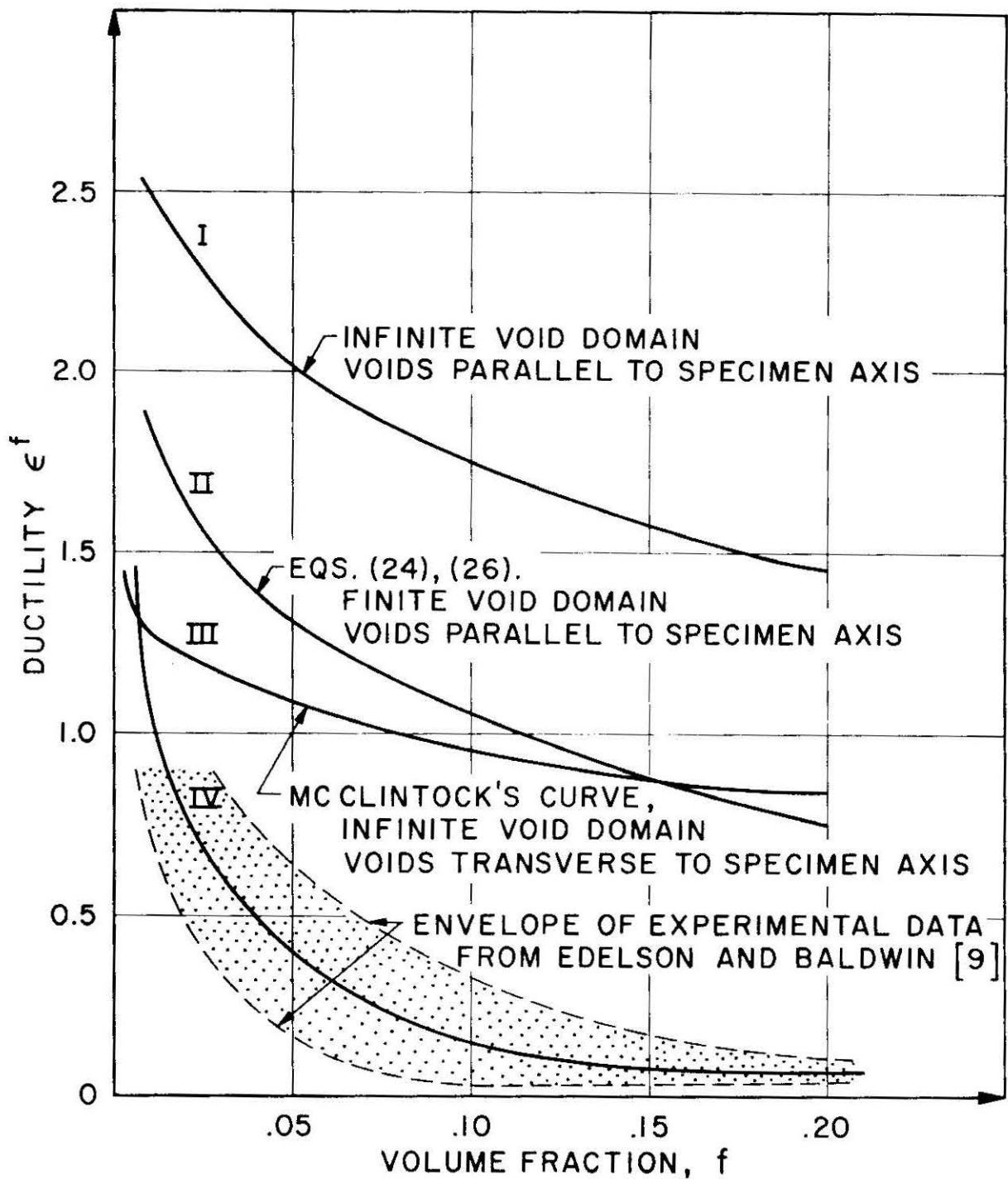


FIG. 8 DUCTILITY VS. INITIAL VOLUME FRACTION OF VOIDS.

affected by interactions among voids. McClintock modeled the neck as composed of cylindrical voids oriented along the three principal directions and entirely neglected interaction. Here interaction is included in an approximate sense but only cylindrical voids parallel to the specimen axis are allowed. A feeling for the effect of void orientation and interaction on ductile fracture can be gained by comparing the various results. The finite and infinite body analyses, curves I and II, show the significant acceleration of void growth, and thus decrease in ductility, due to interactions among voids. The two infinite body analyses, curves I and III, imply that voids transverse to the specimen axis will experience larger growth rates than voids parallel to the axis. A plastic solution to the former case of unequal imposed stresses transverse to the void would be a welcome tool in making further studies (McClintock [5] used an extrapolation from viscous behavior to obtain curve III). The method of approximating void interaction by considering each void growing in a finite body of radius equal to one-half the void spacing cannot be adequately judged until it is built into a complete model of void growth and coalescence. This must allow different orientations of voids and a description of unstable flow between voids. Until then the lower ductility predicted by curve II compared to curve I encourages further thought along these lines.

From the previous two sections we see that the difference in growth rates of voids in perfectly plastic and hardening materials depends directly upon the triaxiality of stress. For the small triaxialities realized in the neck of a tensile specimen it should then be a valid approximation to consider the voids as in a perfectly plastic material. Solving eq. (7) for $N = .0$ gives a very simple relation:

$$(\sigma_r/\tau)_b(\epsilon) = \coth^{-1} \sqrt{1 + \frac{3}{H(\epsilon)^2}} - \coth^{-1} \sqrt{1 + \frac{3}{H(\epsilon)^2} \left(\frac{b}{r_o}\right)^4} \quad (26)$$

The imposed stress state is given by eq. (22); the radius ratio r_o/b is given by eq. (25). Solving eq. (26) for initial void volume fractions from .02 to .2 gives predicted ductilities only a few percent lower than those of eq. (24). Here is a very important simplification of at least the initial growth process of voids in the neck of the tensile specimen. The initial growth can be considered in a perfectly plastic material. Future research will show if the same simplification is possible in the entire growth and coalescence process.

Discussion

The growth of single cylindrical voids in finite and infinite bodies of rigid power-law hardening materials was related to the state of transverse stress, imposed strain, and hardening coefficient. Bounds to the actual flow stress field are presented which release the void growth problem of its dependence on deformation history. By solving two extreme cases, the stress state necessary to maintain an imposed constant growth rate and the growth rate resulting from an imposed constant stress state, the behavior of voids in strain-hardening materials is seen to deviate from perfect plastic behavior directly with value of transverse stress and hardening coefficient. As imposed strain increases the strain-hardening behavior asymptotically approaches perfect plasticity behavior. Small transverse stress states like those in the tensile specimen neck cause little deceleration in growth rate from perfect plastic growth rates.

Although void growth is decelerated directly with hardening coefficient with stress state constant, Rice and Rosengren [10] have shown that there is a rise in stress triaxiality ahead of a crack which is also directly related to hardening coefficient. Since an increase in triaxiality accelerates void growth, hardening could have a net adverse effect on ductility for some configurations.

The theory is applied to the fracture of a tensile specimen by considering the interior of the neck as composed of an array of cylindrical voids oriented parallel to the axis with diameter to spacing ratios equal to the cube root of the initial volume fraction of voids. Considering ductility to be that strain at which the voids' radii grow to one-half the spacing between voids, calculated as if each void were independently growing in a cell of transverse dimension equal to the void spacing, the resulting ductility vs volume fraction curve was very much above the experimental curve of Edelson and Baldwin [9]. Comparing results with McClintock [5] it was concluded that voids normal to the direction of straining grow faster than voids parallel to the axis. Interaction among voids is seen to be a significant factor in void growth from nucleation to coalescence. The need for a more complete model of void growth and coalescence is noted. Such a model would allow random orientation and both stable and unstable interactions among voids. To keep the analysis manageable it seems that only cylindrical and spherical configurations would be included. The problem of the growth of a cylindrical void under unequal transverse stress components must be solved if one chooses to use the cylindrical configuration. The results for the growth of a spherical void in a perfectly plastic material [7] might be utilized. The finite body approximation to interaction could be tested in such a model. Of course the instability of flow between coalescing voids is another problem to be solved.

The tensile specimen fracture problem was solved with the approximation of perfect plastic material with near identical results to the strain-hardening solution. This is a result of the small decelerating effect of hardening at the low triaxial stress states present in the neck. This encourages future work on the tensile test to use the perfect plastic approximation.

Acknowledgment

Sincere gratitude is extended to Professor James R. Rice of Brown University, Mr. Joseph I. Bluhm of the Army Materials and Mechanics Research Center, and Professor Frank A. McClintock of the Massachusetts Institute of Technology for their helpful discussions of the material in this paper. The financial support of the U. S. Atomic Energy Commission, under Contract AT(30-1)-2394 with Brown University, and the assistance of the Army Materials and Mechanics Research Center where the latter portion of this work was accomplished is gratefully acknowledged.

References

1. H. C. Rogers, "Tensile Fracture of Ductile Metals", Trans. Metallurgical Society of AIME, Vol. 218, 1960, pp. 498-506.
2. J. Gurland and J. Plateau, "The Mechanism of Ductile Rupture of Metals Containing Inclusions", Trans. Quarterly of ASM, Vol. 56, 1963, pp. 318-326.
3. J. I. Bluhm and R. J. Morrissey, "Fracture in a Tensile Specimen", Proc. of First International Conference on Fracture, Sendai, Japanese Soc. for Strength and Fracture of Metals, Vol. 3, 1966, pp. 1739-1780.
4. F. A. McClintock and W. R. O'Day, Jr., "Biaxial Tension Distributed Dislocation Cores, and Fracture in Bubble Rafts", Proc. of First International Conference on Fracture, Sendai, Japanese Soc. for Strength and Fracture of Metals, Vol. 1, 1966, pp. 75-98.
5. F. A. McClintock, "On the Mechanics of Fracture from Inclusions", in Ductility, American Soc. for Metals, 1968, pp. 255-278.
6. F. A. McClintock, "A Criterion for Ductile Fracture by the Growth of Holes", Journal of Applied Mechanics, Vol. 35, June 1968, pp. 363-371.
7. J. R. Rice and D. M. Tracey, "On the Ductile Enlargement of Voids in Triaxial Stress Fields", Brown University Report AEC AT(30-1)-2394/33, August 1968.
8. P. W. Bridgman, Studies in Large Plastic Flow and Fracture, McGraw-Hill, New York, 1952.
9. B. I. Edelson and W. M. Baldwin, Jr., "The Effect of Second Phases on the Mechanical Properties of Alloys", Trans. Quarterly ASM, Vol. 55, 1962, pp. 230-250.
10. J. R. Rice and G. F. Rosengren, "Plane Strain Deformation Near a Crack Tip in a Power Law Hardening Material", Journal of the Mech. and Phys. of Solids, Vol. 16, 1968, pp. 1-12.

UNCLASSIFIED

Security Classification

DOCUMENT CONTROL DATA - R&D

(Security classification of title, body of abstract and indexing annotation must be entered when the overall report is classified)

1. ORIGINATING ACTIVITY (Corporate author) Army Materials and Mechanics Research Center Watertown, Massachusetts 02172		2a. REPORT SECURITY CLASSIFICATION Unclassified
		2b. GROUP
3. REPORT TITLE STRAIN-HARDENING AND INTERACTION EFFECTS ON THE GROWTH OF VOIDS IN DUCTILE FRACTURE		
4. DESCRIPTIVE NOTES (Type of report and inclusive dates)		
5. AUTHOR(S) (Last name, first name, initial) Tracey, Dennis M.		
6. REPORT DATE November 1968	7a. TOTAL NO. OF PAGES 28	7b. NO. OF REFS 10
8a. CONTRACT OR GRANT NO.	9a. ORIGINATOR'S REPORT NUMBER(S) AMMRC MS 68-10	
b. PROJECT NO. D/A 1C024401A349	9b. OTHER REPORT NO(S) (Any other numbers that may be assigned this report)	
c. AMCMS Code 5025.11.299		
d. Subtask 39171		
10. AVAILABILITY/LIMITATION NOTICES This document has been approved for public release and sale; its distribution is unlimited.		
11. SUPPLEMENTARY NOTES	12. SPONSORING MILITARY ACTIVITY U. S. Army Materiel Command Washington, D. C. 20315	
13. ABSTRACT The growth and coalescence of voids is a common mechanism of fracture in ductile materials. Analytical work on the problem to date has dealt mainly with isolated voids in perfectly plastic materials, so that strain hardening and interactions between neighboring voids have been neglected. These features of void growth are examined here, but only for a simple geometrical configuration. In particular, the growth of single infinitely long cylindrical voids in bodies of rigid-plastic, strain-hardening material is considered. Bodies with both finite and infinite dimensions normal to the void surface are included in the analysis. The exact relation among the pertinent variables: transverse stress, axial strain, hardening coefficient, void strain and void growth rate is presented. Solution via a bounding technique is given for two general cases. The first case is that of an imposed constant void growth rate and the second case is an imposed constant transverse stress. The results show a decelerating effect of hardening on void growth. Application to the ductile fracture problem of void growth in the neck of a tensile specimen demonstrates the accelerating effect of void growth due to interactions between voids. (Author)		

UNCLASSIFIED

Security Classification

14. KEY WORDS	LINK A		LINK B		LINK C	
	ROLE	WT	ROLE	WT	ROLE	WT
Plastic analysis						
Plasticity						
Ductility						
Fracture (materials)						
Voids						
Strain hardening						
Plastic theory						
Tension tests						
Necking						
Elastic properties						
INSTRUCTIONS						
1. ORIGINATING ACTIVITY: Enter the name and address of the contractor, subcontractor, grantee, Department of Defense activity or other organization (<i>corporate author</i>) issuing the report.	10. AVAILABILITY/LIMITATION NOTICES: Enter any limitations on further dissemination of the report, other than those imposed by security classification, using standard statements such as:					
2a. REPORT SECURITY CLASSIFICATION: Enter the overall security classification of the report. Indicate whether "Restricted Data" is included. Marking is to be in accordance with appropriate security regulations.	<ul style="list-style-type: none"> (1) "Qualified requesters may obtain copies of this report from DDC." (2) "Foreign announcement and dissemination of this report by DDC is not authorized." (3) "U. S. Government agencies may obtain copies of this report directly from DDC. Other qualified DDC users shall request through _____" (4) "U. S. military agencies may obtain copies of this report directly from DDC. Other qualified users shall request through _____" (5) "All distribution of this report is controlled. Qualified DDC users shall request through _____" 					
2b. GROUP: Automatic downgrading is specified in DoD Directive 5200.10 and Armed Forces Industrial Manual. Enter the group number. Also, when applicable, show that optional markings have been used for Group 3 and Group 4 as authorized.						
3. REPORT TITLE: Enter the complete report title in all capital letters. Titles in all cases should be unclassified. If a meaningful title cannot be selected without classification, show title classification in all capitals in parenthesis immediately following the title.						
4. DESCRIPTIVE NOTES: If appropriate, enter the type of report, e.g., interim, progress, summary, annual, or final. Give the inclusive dates when a specific reporting period is covered.						
5. AUTHOR(S): Enter the name(s) of author(s) as shown on or in the report. Enter last name, first name, middle initial. If military, show rank and branch of service. The name of the principal author is an absolute minimum requirement.						
6. REPORT DATE: Enter the date of the report as day, month, year; or month, year. If more than one date appears on the report, use date of publication.						
7a. TOTAL NUMBER OF PAGES: The total page count should follow normal pagination procedures, i.e., enter the number of pages containing information.						
7b. NUMBER OF REFERENCES: Enter the total number of references cited in the report.						
8a. CONTRACT OR GRANT NUMBER: If appropriate, enter the applicable number of the contract or grant under which the report was written.						
8b, 8c, & 8d. PROJECT NUMBER: Enter the appropriate military department identification, such as project number, subproject number, system numbers, task number, etc.						
9a. ORIGINATOR'S REPORT NUMBER(S): Enter the official report number by which the document will be identified and controlled by the originating activity. This number must be unique to this report.						
9b. OTHER REPORT NUMBER(S): If the report has been assigned any other report numbers (<i>either by the originator or by the sponsor</i>), also enter this number(s).						
If the report has been furnished to the Office of Technical Services, Department of Commerce, for sale to the public, indicate this fact and enter the price, if known.						
11. SUPPLEMENTARY NOTES: Use for additional explanatory notes.						
12. SPONSORING MILITARY ACTIVITY: Enter the name of the departmental project office or laboratory sponsoring (<i>paying for</i>) the research and development. Include address.						
13. ABSTRACT: Enter an abstract giving a brief and factual summary of the document indicative of the report, even though it may also appear elsewhere in the body of the technical report. If additional space is required, a continuation sheet shall be attached.						
It is highly desirable that the abstract of classified reports be unclassified. Each paragraph of the abstract shall end with an indication of the military security classification of the information in the paragraph, represented as (TS), (S), (C), or (U).						
There is no limitation on the length of the abstract. However, the suggested length is from 150 to 225 words.						
14. KEY WORDS: Key words are technically meaningful terms or short phrases that characterize a report and may be used as index entries for cataloging the report. Key words must be selected so that no security classification is required. Identifiers, such as equipment model designation, trade name, military project code name, geographic location, may be used as key words but will be followed by an indication of technical context. The assignment of links, rules, and weights is optional.						

UNCLASSIFIED

Security Classification